Extrasynaptic NR2B and NR2D subunits of NMDA receptors shape 'superslow' afterburst EPSC in rat hippocampus

Natasha A. Lozovaya[1], Sergei E. Grebenyuk[1], Timur Sh. Tsintsadze[1], Bihua Feng[2], Daniel T. Monaghan[2] and Oleg A. Krishtal[1]

[1] *Department of Cellular Membranology, Bogomoletz Institute of Physiology, 01024 Kiev, Ukraine and* [2] *Department of Pharmacology, University of Nebraska Medical Center, Omaha, NE 68198, USA*

In conditions of facilitated synaptic release, CA3/CA1 synapses generate anomalously slow NMDA receptor-mediated EPSCs ($EPSC_{NMDA}$). Such a time course has been attributed to the cooperation of synapses through glutamate spillover. Imitating a natural pattern of activity, we have applied short bursts (2–7 stimuli) of high-frequency stimulation and observed a spike-to-spike slow-down of the $EPSC_{NMDA}$ kinetics, which accompanied synaptic facilitation. It was found that the early component of the $EPSC_{NMDA}$ and the burst-induced late component of the $EPSC_{NMDA}$ have distinct pharmacological properties. The competitive NMDA antagonist *R*-(−)-3-(2-carboxypiperazine-4-yl)-propyl-1-phosphonic acid (*D*-CPP), which has higher affinity to NR2A than to NR2B subunits and lowest affinity at NR2D subunits, significantly slowed down the decay rate of the afterburst EPSC while leaving the kinetics of the control current unaffected. In contrast, ifenprodil, a highly selective NR2B antagonist, and [±]-*cis*-1-[phenanthren-2yl-carbonyl]piperazine-2,3-dicarboxylic acid (PPDA), a competitive antagonist that is moderately selective for NR2D subunits, more strongly inhibited the late component of the afterburst $EPSC_{NMDA}$. The receptors formed by NR2B and (especially) NR2D subunits are known to have higher agonist sensitivity and much slower deactivation kinetics than NR2A-containing receptors. Furthermore, NR2B is preferentially and NR2D is exclusively located on extrasynaptic membranes. As the density of active synapses increases, the confluence of released glutamate makes EPSC decay much longer by activating more extrasynaptic NR2B- and NR2D-subunit-containing receptors. Long-term potentiation (LTP) induced by successive rounds of burst stimulation is accompanied by a long-term increase in the contribution of extrasynaptic receptors in the afterburst $EPSC_{NMDA}$.

(Resubmitted 5 March 2004; accepted after revision 10 May 2004; first published online 14 May 2004)
Corresponding author O. A. Krishtal: Department of Cellular Membranology, Bogomoletz Institute of Physiology, 01024 Kiev, Ukraine. Email: krishtal@serv.biph.kiev.ua

The spillover of synaptically released Glu described in numerous studies is important in the understanding of information processing in the hippocampus. The reason for this is straightforward. Since spillover implies intersynaptic cross-talk, the question is, whether such a highly cooperative synaptic system is capable of retaining address specificity in the processing of information. When studied *in vitro*, cooperative behaviour of CA3/CA1 synapses is displayed by the generation of the slow NMDA receptor-mediated EPSCs ($EPSC_{NMDA}$) with kinetics dependent on the number of activated synapses. When this number is increased (or, alternatively, Glu uptake inhibited), $EPSC_{NMDA}$ becomes progressively slower, reaching durations in the range of seconds (Lozovaya *et al.* 1999; Arnth-Jensen *et al.* 2002). Interpreted in terms of spillover, such a duration implies the diffusion of released Glu well beyond immediately neighbouring synapses and its cooperative confluence on distant postsynaptic and extrasynaptic sites, which results in much delayed activation of receptors (Arnth-Jensen *et al.* 2002).

CA1 pyramidal cells express mRNA for three different NR2 NMDA receptor subunits: NR2A, NR2B and NR2D. This has been shown in adult humans (Scherzer *et al.* 1998) and in juvenile rats (Kirson *et al.* 1999; Hrabetova *et al.* 2000). Co-expression of NMDAR1 with one or more of the NR2 subunits generates receptors with distinct functional and pharmacological properties (Kutsuwada

 DOI: 10.1113/jphysiol.2004.063792

et al. 1992; Monyer *et al.* 1994; Vicini *et al.* 1998). Thus, deactivation times for diheteromeric NMDARs differ in a 50-fold range, following the sequence: NR2A < 2C = 2B ≪ 2D. The deactivation time constant for the macroscopic current mediated by NR1/NR2A assemblies comprises tens of milliseconds, compared to hundreds of milliseconds for NR1/NR2B and several seconds for NR1/NR2D receptors (Monyer *et al.* 1994; Vicini *et al.* 1998; Wyllie *et al.* 1998; Cull-Candy *et al.* 2001). The subunit composition of extrasynaptic and synaptic NMDA receptors in mature hippocampal neurones is asymmetrical: synaptic NMDA receptors contain NR2A (predominantly) and NR2B subunits, whereas extrasynaptic NMDA receptors contain mostly NR2B subunits (Tovar & Westbrook, 1999). Native NR2D subunit-incorporated receptors have been identified only extrasynaptically. There is no evidence so far for NR2D-containing receptors at any central synapse (Momiyama *et al.* 1996; Cull-Candy *et al.* 1998; Cull-Candy *et al.* 2001). It has been shown recently that NR2D-containing receptors are clearly present in the adult hippocampus (Thompson *et al.* 2002). Importantly, NR2D subunit-like immunoreactivity is evident in the dendrites of CA1 pyramidal cells. Pharmacological data indicate that several NMDA receptor blockers have differential selectivities among the various subunits of this receptor. Since the extrasynaptic receptors are expected to be much slower than the postsynaptic ones, their increased activity (as a consequence of spillover) should contribute to the 'superslow' kinetics of the EPSC. Using available pharmacological agents, we have tested this hypothesis.

Methods

Preparation of hippocampal slices

This study was carried out on Wistar rats (21 days old, WAG/GSto, Moscow, Russia). All experiments were performed in accordance with the guidelines of the Institutional Animal Care and Use Committee (protocol no. 2/0204). After decapitation, rat brains were immediately transferred to a chilled (4°C) solution of the following composition (mM): 120 NaCl, 5 KCl, 26 $NaHCO_3$, 2 $MgCl_2$, 0.5 $CaCl_2$ and 20 glucose. The solution was constantly equilibrated with a gas mixture of 95% O_2–5% CO_2 to maintain a pH of 7.4. During the pre-incubation, the slices (300–400 μm thick) were kept fully submerged in the extracellular solution (mM): 135 NaCl, 5 KCl, 26 $NaHCO_3$, 1.5 $CaCl_2$, 1.5 $MgCl_2$ and 20 glucose (pH 7.4, equilibrated with 95% O_2–5% CO_2). The experiments were conducted in a similar solution, but containing 2 mM $CaCl_2$ and 1 mM $MgCl_2$, at 32–34°C. Picrotoxin (50 μM) and (2*S*)-(+)-5,5-dimethyl-2-morpholineacetic acid (SCH 50911) (10 μM) were added to the extracellular solution to suppress inhibitory activity of interneurones.

Electrophysiological recordings in hippocampal slices

A standard whole-cell patch clamp technique was used to record EPSCs from CA1 pyramidal neurones *in situ* in response to stimulation of the Schaffer collateral–commissural pathway. To prevent the spread of electrical activity from area CA3, mini-slices were prepared by making a cut orthogonal to the stratum pyramidale and extending to the mossy fibres layer. Intracellular solution for patch pipettes contained (mM): 100 $TrisPO_4$ or CsF, 40 NaH_2PO_4, 10 Hepes-CsOH and 10 Tris-Cl (pH 7.2). pH was adjusted with Tris OH or CsOH *N*-(2,6-dimethyl-phenylcarbamoylmethyl)-triethylammonium bromide (QX-314; 2–3 mM) was routinely added to the intracellular solution to block voltage-gated sodium conductance. Patch pipettes were pulled from soft borosilicate glass on a two-stage horizontal puller. When fire polished and filled with the intracellular solution, they had a resistance of 2–3 MΩ. Currents were digitally sampled at 400 μs intervals by a 12-digit ADC board and filtered at 3 kHz. Access resistance was monitored throughout the experiments and ranged typically from 6 to 9 MΩ. When the access resistance was changed by more than 25% during the experiment, the data were discarded. To stimulate the Schaffer collateral–commissural pathway, a bipolar Ni–Cr electrode was positioned on the surface of the slice. The current intensity of test stimuli (25–50 μA) was set to produce half-maximal EPSPs. Current pulses were delivered through the isolated stimulator HG 203 (Hi-Medical, London, UK) at 0.066–0.2 Hz. Student's unpaired *t* test was used for statistical analysis. Data are expressed as means ± S.E.M. Field potential recordings were conducted using tungsten electrode. Population spikes were measured in stratum pyramidale and field EPSPs were measured in stratum radiatum. Pharmacologically isolated $EPSP_{NMDA}$ was recorded in a modified extracellular solution containing 0.5 mM Mg^{2+} and 2.5 mM Ca^{2+} in the presence of 2,3-dioxo-6-nitro-1,2,3,4-tetrahydrobenzo[f] quinoxaline-7-sulphonamide (NBQX).

NR subunit expression in *Xenopus* oocytes

cDNA encoding the NMDAR1a subunit was a generous gift of Dr Shigetada Nakanishi (Kyoto, Japan). cDNA encoding the NR2A, NR2C and NR2D were kindly provided by Dr Peter Seeburg (Heidelburg, Germany)

and the NR2B [5′UTR] cDNA was the generous gift of Drs Dolan Pritchett and David Lynch (Philadelphia, PA, USA). Plasmids were linearized with *Not* I (NR1a), *Eco*R I (NR2A, NR2C and NR2D) or *Sal* I (NR2B) and transcribed *in vitro* with T3 (NR2A and NR2C), SP6 (NR2B) or T7 (NR1a and NR2D) RNA polymerase using the mMessage mMachine Transcription Kits (Ambion, Austin, TX, USA).

Oocytes were removed from mature female *Xenopus laevis* (Xenopus One, Ann Arbor, MI, USA) under anaesthesia as previously described (Buller *et al.* 1994). The frogs were humanely killed after the final collection. NMDA receptor subunit RNAs were dissolved in sterile distilled H_2O. NR1a and NR2 RNAs were mixed in a molar ratio of 1:3. Fifty nanolitres of the final RNA mixture was microinjected (15–30 ng in total) into the oocyte cytoplasm. Oocytes were incubated in ND-96 oocyte culture medium (96 mM NaCl, 2 mM KCl, 1–8 mM $CaCl_2$, 1 mM $MgCl_2$, 5 mM Hepes) at 17°C prior to electrophysiological assay (1–5 days).

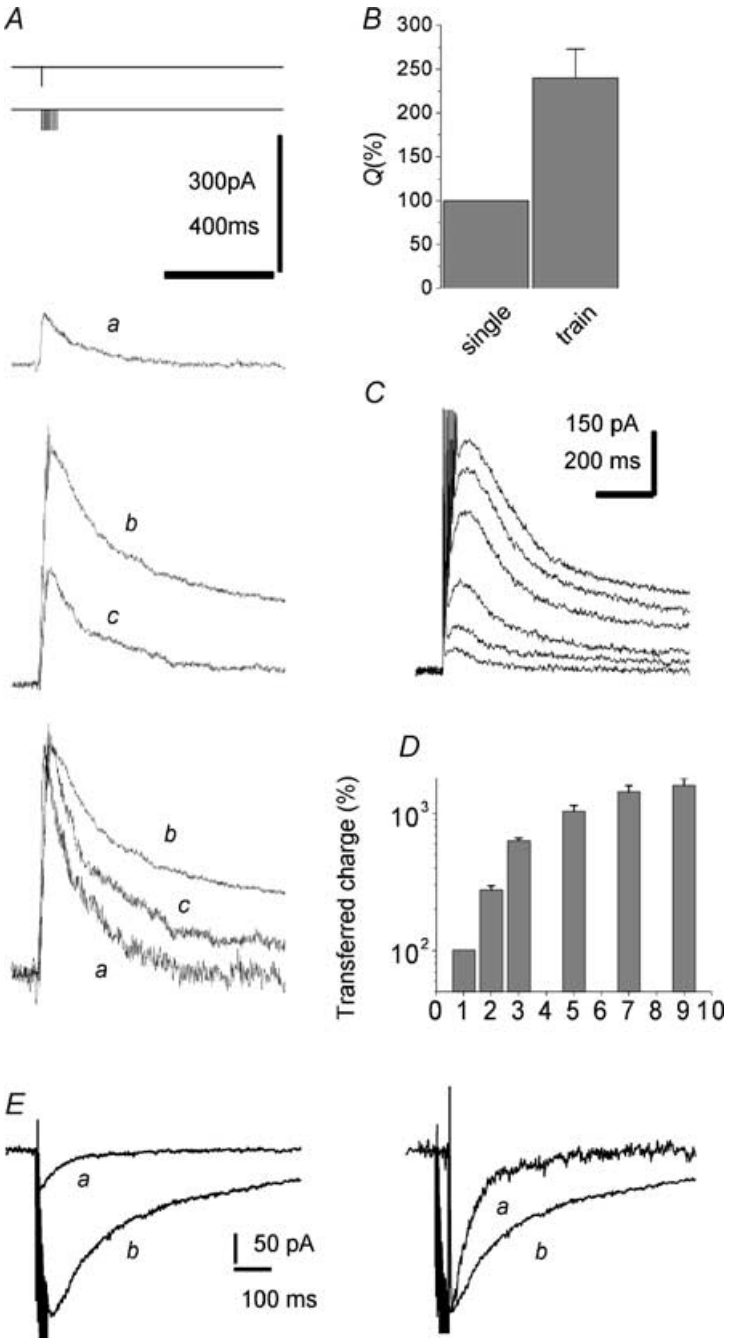

Figure 1. Superslow $EPSC_{NMDA}$ elicited by short trains of stimulation applied to the Schaffer collateral–commissural pathway

The transferred charge depends on the number of stimuli within a short train. *A*, $EPSC_{NMDA}$ was induced by a single pulse ($EPSC^{single}_{NMDA}$, trace *a*) and by 7 pulses at 200 Hz ($EPSC^{train}_{NMDA}$, trace *b*). Trace *c* was obtained at a lower stimulus intensity (50% of control) than trace *b*. Holding voltage +50 mV. Here and hereafter, stimulation protocols are schematically represented over the traces; the peak amplitude of the $EPSC_{NMDA}$ has been measured as the mean over a 10 ms window around the peak. *B*, the averaged charge transferred by the $EPSC^{single}_{NMDA}$ and $EPSC^{train}_{NMDA}$ both normalized to the corresponding current peak amplitude. Here and hereafter, charge normalized to the peak amplitude is indicated as Q = charge/amplitude. The value obtained for the $EPSC^{single}_{NMDA}$ is taken as 100%. *C*, the $EPSC^{train}_{NMDA}$ elicited by a progressively increasing number of stimuli (from 1 to 9). Larger and slower traces correspond to a larger number of stimuli. *D*, charge transferred by the $EPSC^{train}_{NMDA}$ as a function of stimuli number. *E*, representative traces of the $EPSC_{NMDA}$ induced by a single pulse (*a*) and by 7 pulses at 200 Hz (*b*) recorded at a holding potential of −45 mV. Traces on left are normalized.

Electrophysiological recordings in *Xenopus* oocytes

Electrophysiological responses were measured using a standard two-microelectrode voltage clamp as previously described (Buller & Monaghan, 1997). The recording buffer contained (mM): 116 NaCl, 2 KCl, 2 $BaCl_2$ and 5 Hepes, pH 7.4 (adjusted with NaOH). Response magnitude was determined by the steady plateau response elicited by bath application of 10 μM L-glutamate plus 10 μM glycine at a holding potential of −60 mV. Response amplitudes for the four heteromers were generally between 30 and 100 nA. Attempts were made to keep response magnitudes within this range to minimize activation of the endogenous Cl^- current. The presence of a plateau response was taken as an indication of the lack of significant activation of the endogenous Cl^- current by Ba^{2+} in these cells. Antagonist inhibition curves were fitted (GraphPad Prism, ISI Software, San Diego, CA, USA) according to the equation, $I = I_{max} - I_{max}/[1 + (IC_{50}/A)^n]$, where I_{max} is the current response in the absence of antagonist, A is the antagonist concentration and IC_{50} is the antagonist concentration producing half-maximal inhibition. Apparent K_i values were determined by correcting for agonist affinity according to the equation, $IC_{50} = IC_{50}(obs)/1 + ([agonist]/EC_{50})$, as described by Durand *et al.* (1992). ANOVA with a Newman–Keuls multiple comparison test was used for statistical analysis. Data are expressed as means ± S.E.M.

Drugs

Sodium bicarbonate and CsF were obtained from Merck (Darmstadt, FRG); lidocaine QX-314 and picrotoxin were purchased from RBI (Natick, MA, USA); and 6-nitro-7-sulphamoylbenzo[f]quinoxalin-2,3-dione (NBQX) was obtained from Tocris Cookson (Bristol, UK). All other chemicals were from Sigma (St Louis, MO, USA).

Results

The NMDA receptor-mediated component of the EPSC was measured in CA1 pyramidal cells in response to Schaffer collateral–commissural pathway stimulation in the presence of NBQX (10 μM). We applied short bursts (2–9 stimuli) of high-frequency stimulation that imitate natural stimulus patterns (Dobrunz & Stevens, 1999). Measurements were performed at a holding voltage of

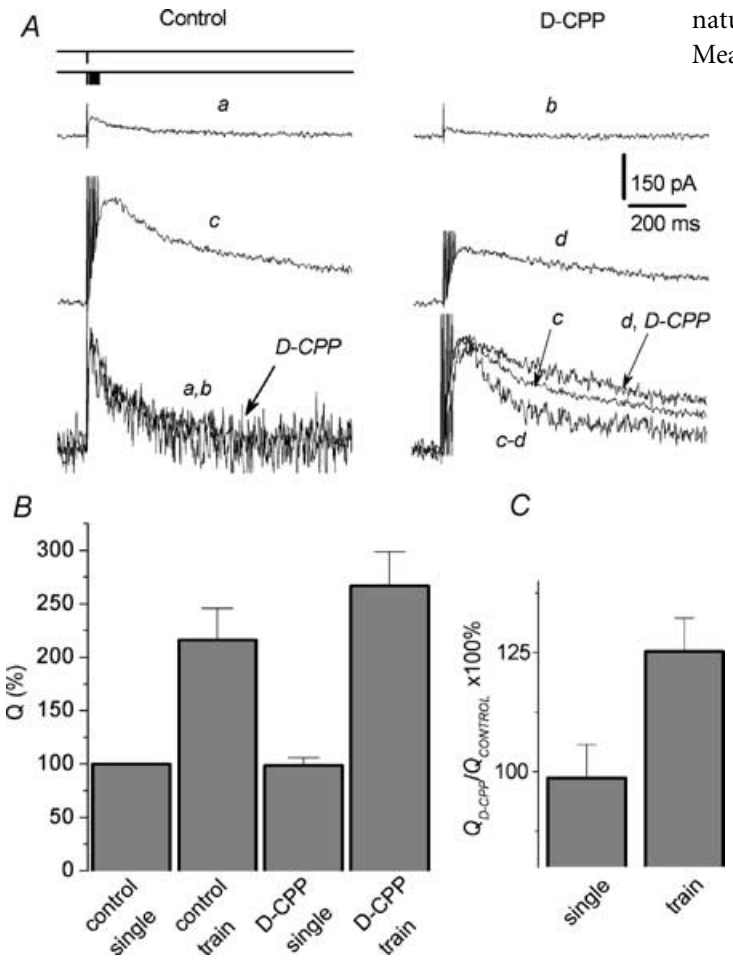

Figure 2. Delayed component of the afterburst EPSC displays lower sensitivity to *D*-CPP
A, the late component of the $EPSC^{train}_{NMDA}$ was inhibited by *D*-CPP much less than the current at the peak. The $EPSC_{NMDA}$ was evoked by a single pulse (trace *a,* control; *b,* with *D*-CPP), and by a 7 pulse train (trace *c,* control; *d,* with *D*-CPP; 200 Hz). Holding voltage was +50 mV. Lower line: corresponding traces normalized and superimposed; *c* and *d*, the subtraction of currents before and after application of *D*-CPP (normalized after subtraction). *D*-CPP does not alter the kinetics of the $EPSC^{single}_{NMDA}$, but slows down the kinetics of the $EPSC^{train}_{NMDA}$. *B*, the charge transferred by the $EPSC^{single}_{NMDA}$ and the $EPSC^{train}_{NMDA}$ normalized to the corresponding peak current amplitude recorded in control solution and in the presence of *D*-CPP. The value of *Q* obtained for the control $EPSC^{single}_{NMDA}$ was taken as 100%. *C*, the ratio of normalized to the peak amplitude charges transferred by the $EPSC_{NMDA}$ recorded with and without *D*-CPP; calculated as $\frac{Q_{D-CPP}}{Q_{Control}}$.

+50 mV (Fig. 1*A–D*). In parallel, the experiments were performed at a holding voltage of −45 mV with similar results (Fig. 1*E*).

The strength of the stimulus was adjusted to maintain the EPSC amplitudes in the range of 100–500 pA. In previous studies (Diamond, 2001; Arnth-Jensen *et al.* 2002) such amplitudes of current were shown not to be connected with major failures of voltage clamp that could at least qualitatively distort the changes in the EPSC time course.

When measured after a short train of stimuli (typically 7 stimuli applied at 200 Hz), the $EPSC_{NMDA}$ ($EPSC^{train}_{NMDA}$) was considerably facilitated, while its decay was dramatically slowed down. (Fig. 1*A*, traces *a* and *b*). This observation is in complete agreement with earlier data (Arnth-Jensen *et al.* 2002). The time course of alterations in the $EPSC^{train}_{NMDA}$ were quantified by normalizing the charge transfer with the peak amplitude of the $EPSC_{NMDA}$ (measured as mean over 10 ms window around the peak). A larger charge transfer corresponds to slower decay kinetics and vice versa. Normalized charge transfer of the $EPSC^{train}_{NMDA}$ was $240 \pm 32\%$ ($P < 0.001$, $n = 32$, Fig. 1*B*) of the same parameter for the $EPSC_{NMDA}$ induced by a single stimulus ($EPSC^{single}_{NMDA}$). Correspondingly, the half-decay time of $EPSC^{single}_{NMDA}$ was 124 ± 20 ms, while the same value of the $EPSC^{train}_{NMDA}$ was 428 ± 73 ms. The mean ratio of these parameters was $400 \pm 96\%$, $P < 0.002$, $n = 32$.

For a given number of stimuli, the larger the stimulus applied, the greater this effect becomes (Fig. 1*A* traces *b* and *c*). Such behaviour is consistent with the spillout of L-glutamate from the synaptic cleft (Asztely *et al.* 1997; Diamond, 2001; Arnth-Jensen *et al.* 2002).

In many functional and behavioural states, natural spiking patterns in the brain are composed of relatively short periods of high-frequency activity. Specifically in hippocampus, pyramidal cells frequently have two to nine action potentials fired at frequencies up to 200 Hz (Kandel & Spencer, 1961; Rank, 1973; Suzuki & Smith, 1985). How significant is every spike within this small number? To address this question, we analysed the changes in the time course of EPSCs by varying the number of stimuli in the 200 Hz train. Figure 1*C* demonstrates that the gradual change in the $EPSC_{NMDA}$ kinetics becomes notable, starting

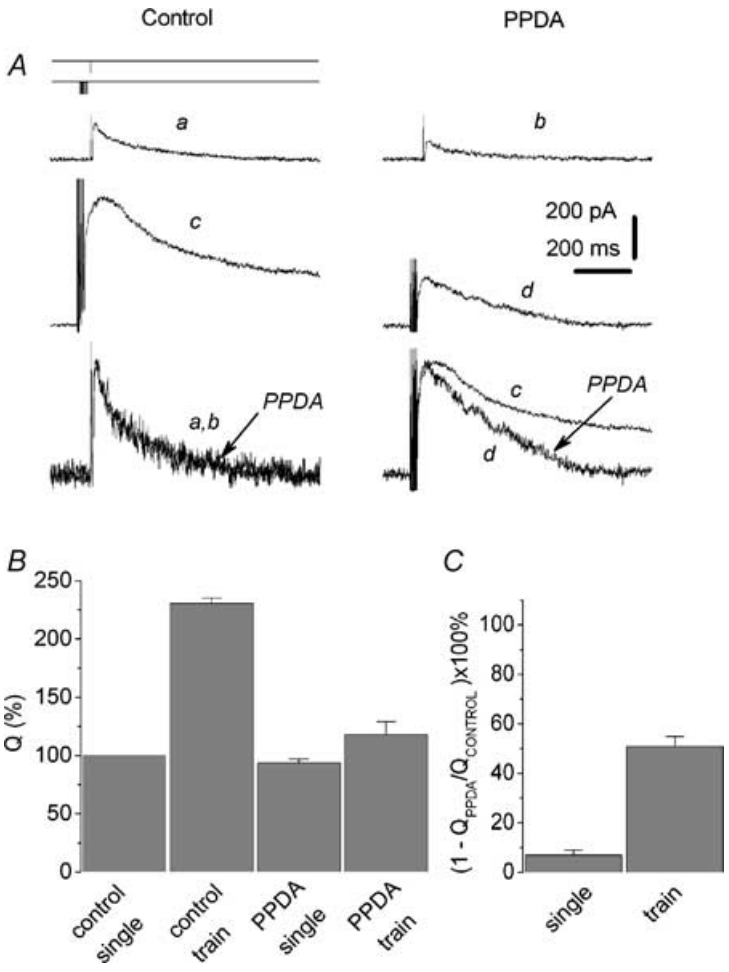

Figure 3. Delayed component of the $EPSC^{train}_{NMDA}$ has higher sensitivity to PPDA than the $EPSC^{single}_{NMDA}$
A, Upper traces: the $EPSC_{NMDA}$ evoked by a single pulse (traces *a* and *b*) and by a train 7 pulses long (traces *c* and *d*, 200 Hz) in control conditions (traces *a* and *c*) and with (±) *cis*-1-(phenanthren-2yl-carbonyl) piperazine-2,3-dicarboxylic acid (PPDA) (traces *b* and *d*). The late component of the $EPSC^{train}_{NMDA}$ has a higher sensitivity to PPDA compared to the peak. Holding voltage was +50 mV. Lower traces: corresponding traces normalized and superimposed. *B*, the charge transfer of the $EPSC^{single}_{NMDA}$ and the $EPSC^{train}_{NMDA}$ normalized to the corresponding peak current amplitude; recordings in control solution and in the presence of PPDA. The *Q* value for the control $EPSC^{single}_{NMDA}$ was taken as 100%. *C*, the contribution of the PPDA-sensitive component ($Q_{Control} - Q_{PPDA}$) to the $EPSC^{single}_{NMDA}$ and the $EPSC^{train}_{NMDA}$ (calculated as $1 - \frac{Q_{PPDA}}{Q_{Control}}$).

even from the second stimulus. The dependence of the charge transferred by $EPSC_{NMDA}$ on the number of spikes in the short presynaptic burst is demonstrated in Fig. 1*D*. The saturation of the effect is observed after seven to nine stimuli. This indicates that a further increase in the number of stimuli would have negligible impact on NMDA receptor-mediated calcium signalling in a postsynaptic neurone.

Binary complexes of NMDA receptors composed of NR1 and NR2D subunits have been shown to display unique electrophysiological behaviour, including highest affinity for both glutamate and glycine (Ikeda *et al.* 1992), as well as extremely slow current deactivation (Monyer *et al.* 1994; Vicini *et al.* 1998), which fits well the time scale of decay of the afterburst EPSC. We therefore hypothesized that the extremely slow time course of the facilitated EPSC is due to the spillover of Glu and the subsequent activation of slowly deactivating extrasynaptic NR2B-containing receptors and NR2D-containing receptors. To check this hypothesis we used agents which preferentially block various NMDA receptor subunits. Thus, NR2D subunit-incorporating NMDA receptor can be distinguished by the competitive NMDA receptor antagonist *D*-CPP, which has a high preference for NR2A/B over NR2D subunits (Beaton *et al.* 1992; Buller *et al.* 1994). *D*-CPP K_i values were evaluated for recombinant NR2 subunits coexpressed with NR1a subunits in *Xenopus* oocytes. The corresponding K_i values were: NR2A, 41 ± 3 nM; NR2B, 270 ± 20 nM; NR2C, 630 ± 50 nM; and NR2D, 1990 ± 200 nM. NR2D affinity was statistically different from each of the other heterodimers by $P < 0.001$, $n = 5$.

Figure 2*A–C* demonstrates that the delayed component of the $EPSC^{train}_{NMDA}$ is more weakly inhibited by *D*-CPP than the current at the peak, while there is no change in the kinetics of $EPSC^{single}_{NMDA}$. In the presence of *D*-CPP ($1\ \mu$M), normalized charge transfer for the $EPSC^{train}_{NMDA}$ comprised $125 \pm 7\%$ of control values, *versus* $98 \pm 7\%$ for corresponding parameters for $EPSC^{single}_{NMDA}$ ($P < 0.02$, $n = 7$, Fig. 2*C*). Correspondingly, *D*-CPP did not change $t_{1/2}$ of $EPSC^{single}_{NMDA}$ ($110 \pm 10\%$ of control), while $t_{1/2}$

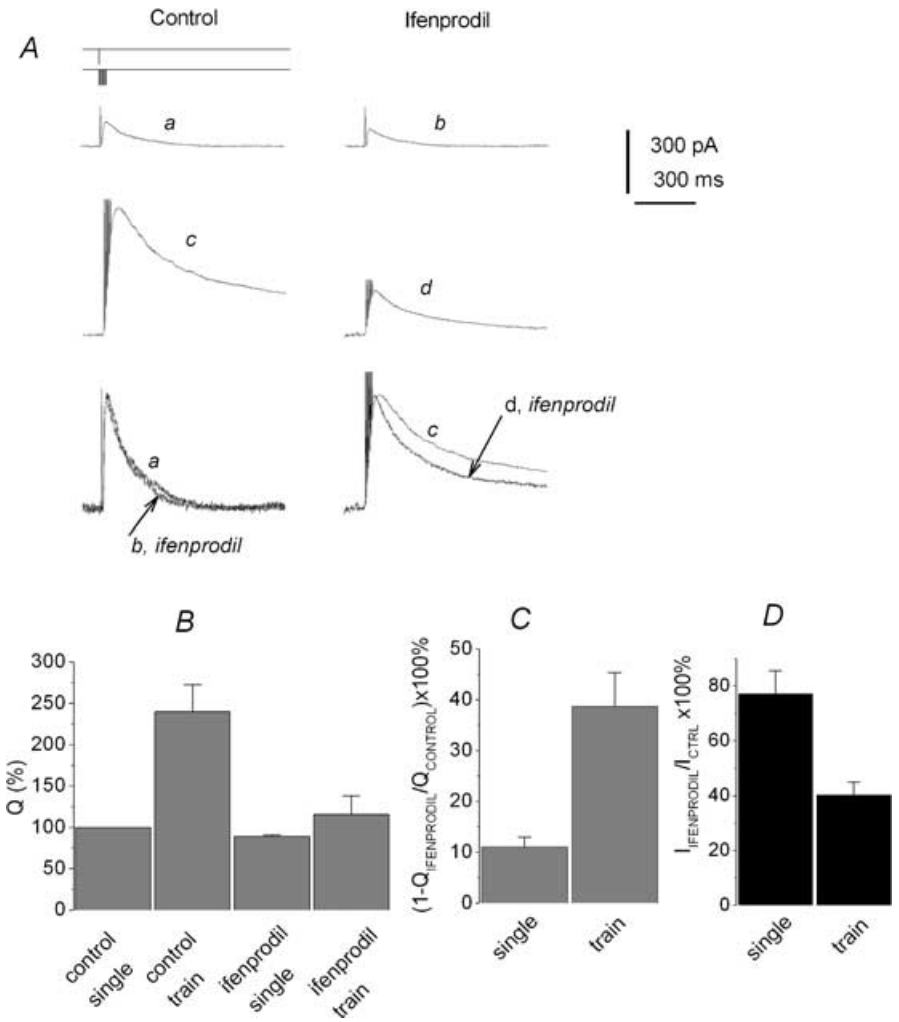

Figure 4. Increased contribution of the ifenprodil-sensitive component to the afterburst $EPSC_{NMDA}$
A, ifenprodil accelerates the decay of the $EPSC^{train}_{NMDA}$. Partial block by ifenprodil of the $EPSC_{NMDA}$ induced by a single pulse (traces *a* and *b*) and by 7 pulses at 200 Hz (traces *c* and *d*) with (traces *b* and *d*) and without (traces *a* and *c*) ifenprodil. Holding voltage was +50 mV (A). Lower traces: the traces normalized and superimposed. *B*, the charge transfer for the $EPSC^{single}_{NMDA}$ and the $EPSC^{train}_{NMDA}$ normalized to the corresponding current peak amplitude; recordings were made in control solution and in the presence of ifenprodil. The *Q* value obtained for the control $EPSC^{single}_{NMDA}$ was taken as 100%. *C*, contribution of the ifenprodil-sensitive component ($Q_{Control} - Q_{Ifenprodil}$) to the $EPSC^{single}_{NMDA}$ and the $EPSC^{train}_{NMDA}$ (calculated as $1 - \frac{Q_{Ifenprodil}}{Q_{Control}}$). *D*, enhancement of the block induced by ifenprodil at the peak of the $EPSC^{train}_{NMDA}$. Effect of ifenprodil on the peak value of $EPSC_{NMDA}$ evoked by single stimuli and trains.

of $EPSC^{train}_{NMDA}$ was increased up to $166 \pm 20\%$ ($n = 7$; $P < 0.02$). These changes reflect much slower kinetics of the $EPSC^{train}_{NMDA}$ decay under the action of *D*-CPP. Since the expression of NR2C-incorporating receptors has not been detected in the hippocampus of rats at this age (Kirson *et al.* 1999), this result could indicate the increased contribution of NR2D receptors in conditions of enhanced glutamate release. If this hypothesis is correct, then preferential inhibition of NR2D receptors over NR2A/B receptors would result in the opposite effect, that is acceleration of the $EPSC^{train}_{NMDA}$ decay. Although antagonists highly selective for NR2D-containing receptors have not been described, PPDA demonstrates a small, but significant, preference for blocking NR2D-containing NMDA receptors compared to NR2A- and NR2B-containing receptors. PPDA K_i values for inhibiting the responses of recombinant NMDA receptors expressed in *Xenopus* oocytes are (nM): 680 ± 170 for NR1a/NR2A; 350 ± 2 for NR1a/NR2B; 70 ± 15 for NR1a/NR2C; and 108 ± 32 for NR1a/NR2D receptors (Hrabetova *et al.* 2000).

We have found that PPDA (10 μM) strongly accelerates the decay rate of the $EPSC^{train}_{NMDA}$ (Fig. 3). Correspondingly, the normalized charge transfer produced by the PPDA-sensitive component of the $EPSC^{train}_{NMDA}$ was $51 \pm 6\%$ of control values, while the corresponding value for the $EPSC^{single}_{NMDA}$ was only $7 \pm 2\%$, $P < 0.004$, $n = 7$ (Fig. 3*B* and *C*). PPDA did not alter $t_{1/2}$ of $EPSC^{single}_{NMDA}$ ($101 \pm 22\%$ of control), while $t_{1/2}$ of $EPSC^{train}_{NMDA}$ was decreased to $29 \pm 9\%$ ($n = 5$; $P < 0.04$). The concentration of PPDA used in this set of experiments was higher than those that follow from K_i values for inhibiting the responses of recombinant NMDA receptors expressed in *Xenopus* oocytes. The concentration of PPDA used in these experiments was in a good agreement with those that follow from K_i values for inhibiting the responses of recombinant NMDA receptors expressed in oocytes, despite the fact that the K_i values obtained from oocyte data cannot be entirely extrapolated

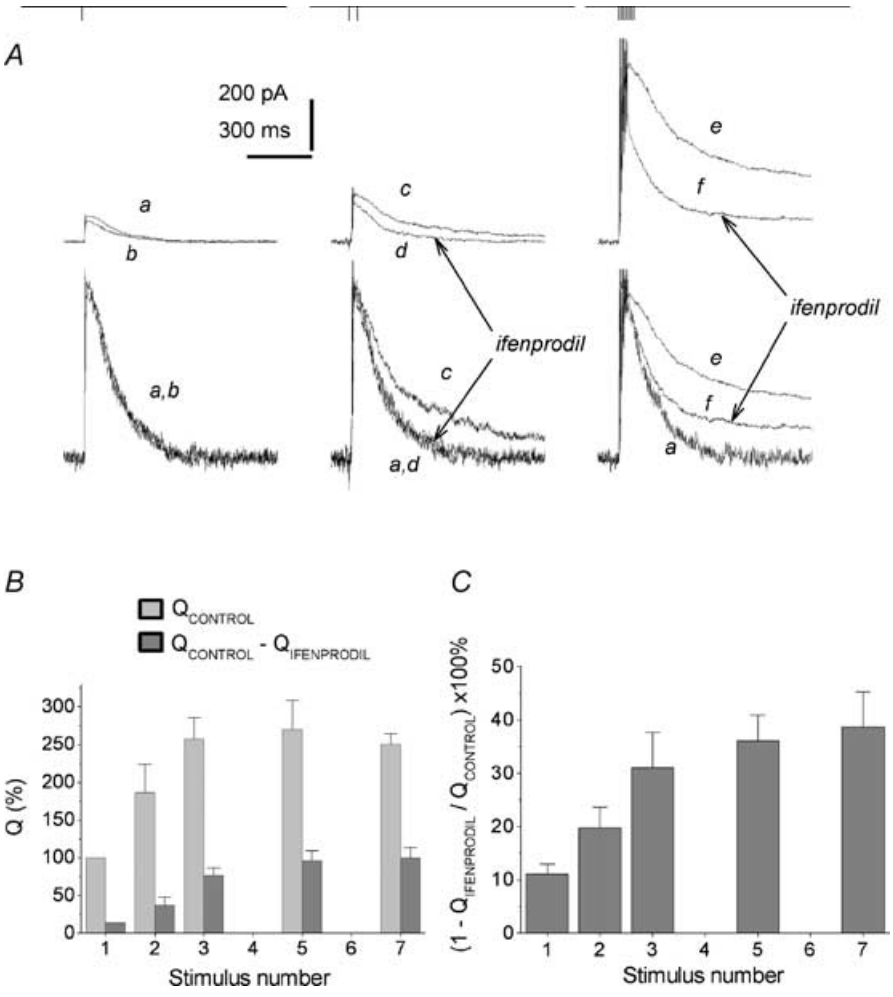

Figure 5. The contribution of the ifenprodil-sensitive component to the $EPSC^{train}_{NMDA}$ depends on the number of spikes in a burst

A, the slow-down of the $EPSC_{NMDA}$ decay rate on a spike-to-spike basis. Upper traces: $EPSC_{NMDA}$ evoked by a single pulse (traces *a* and *b*), 2 pulses (traces *c* and *d*) and 7 pulses (traces *e* and *f*) of 200 Hz stimulation, recorded in control solution (traces *a, c* and *e*) and in the presence of ifenprodil (traces *b, d* and *f*). Holding voltage was +50 mV. Lower traces: corresponding traces normalized and superimposed. *B*, the charge transferred by control $EPSC_{NMDA}$ and the ifenprodil-sensitive component $EPSC_{NMDA}$ ($Q_{Control} - Q_{Ifenprodil}$) evoked by a progressively increasing number of pulses (from 1 to 7) in the train (200 Hz). The value obtained for $EPSC^{single}_{NMDA}$ measured in control is taken as 100%. *C*, the contribution of the ifenprodil-sensitive component to the $EPSC_{NMDA}$ as a function of stimulation pulse number (from 1 to 7), 200Hz train (calculated as $1 - \frac{Q_{Ifenprodil}}{Q_{Control}}$).

to the slice experiments as the compound may possibly exhibit limited penetration into the brain tissue. In some experiments, the concentration of PPDA was empirically chosen to induce a significant (~50%) block of the peak EPSC.

The acceleration of $EPSC^{train}_{NMDA}$ decay by PPDA may be mediated at least partly by the inhibition of NR2B subunit-containing receptors. However, elimination of the superslow (of the order of seconds) component of $EPSC^{train}_{NMDA}$ (see Fig. 3*A*, traces *c* and *d*) further indicates the involvement of NR2D receptors.

Recently it has been demonstrated that in hippocampal pyramidal neurones NMDA receptors containing the NR2A subunit localize preferentially at synaptic sites, while the distribution of NR2B receptors is mostly extrasynaptic (Tovar & Westbrook, 1999). Both types of receptors are activated by stimulation of the Schaffer collateral–commissural pathway in hippocampal slices of adult mice (Kirson & Yaari, 1996). The non-competitive antagonist ifenprodil effectively inhibits NR1/NR2B channels ($IC_{50} = 0.34\,\mu M$), whereas the NR1/NR2A channels are inhibited with 400-fold lower affinity ($IC_{50} = 146\,\mu M$) (Williams, 1993). Another NR2B-containing NMDA receptor, NR1/NR2A/NR2B, demonstrates intermediate affinity to ifenprodil (Kew *et al.* 1998).

According to the spillover hypothesis, the contribution of predominantly extrasynaptic NR2B subunit-containing receptors to the aftertrain EPSC should increase in the same manner as for NR2D subunit-containing receptors. Indeed, the delayed component of the $EPSC^{train}_{NMDA}$ was inhibited by ifenprodil ($30\,\mu M$) much stronger than the current in the peak (Fig. 4 traces *c* and *d*). The normalized charge transfer produced by the ifenprodil-sensitive component of the $EPSC^{train}_{NMDA}$ was $39 \pm 3\%$ of control values, while the corresponding value for the $EPSC^{single}_{NMDA}$ was $11 \pm 2\%$ ($P < 0.001$, $n = 7$, Fig. 4*B* and *C*). Correspondingly, ifenprodil only slightly altered $t_{1/2}$ of $EPSC^{single}_{NMDA}$ ($91 \pm 5\%$ of control), while $t_{1/2}$ of $EPSC^{train}_{NMDA}$ was decreased to $45 \pm 5\%$ ($n = 7$; $P < 0.02$).

It should be specifically noted that the non-competitive antagonist ifenprodil inhibits the peak of the $EPSC^{train}_{NMDA}$ more strongly than $EPSC^{single}_{NMDA}$ ($40 \pm 2\%$ for $EPSC^{train}_{NMDA}$ *versus* $77 \pm 4\%$ for $EPSC^{single}_{NMDA}$, $P < 0{,}001$, $n = 7$,

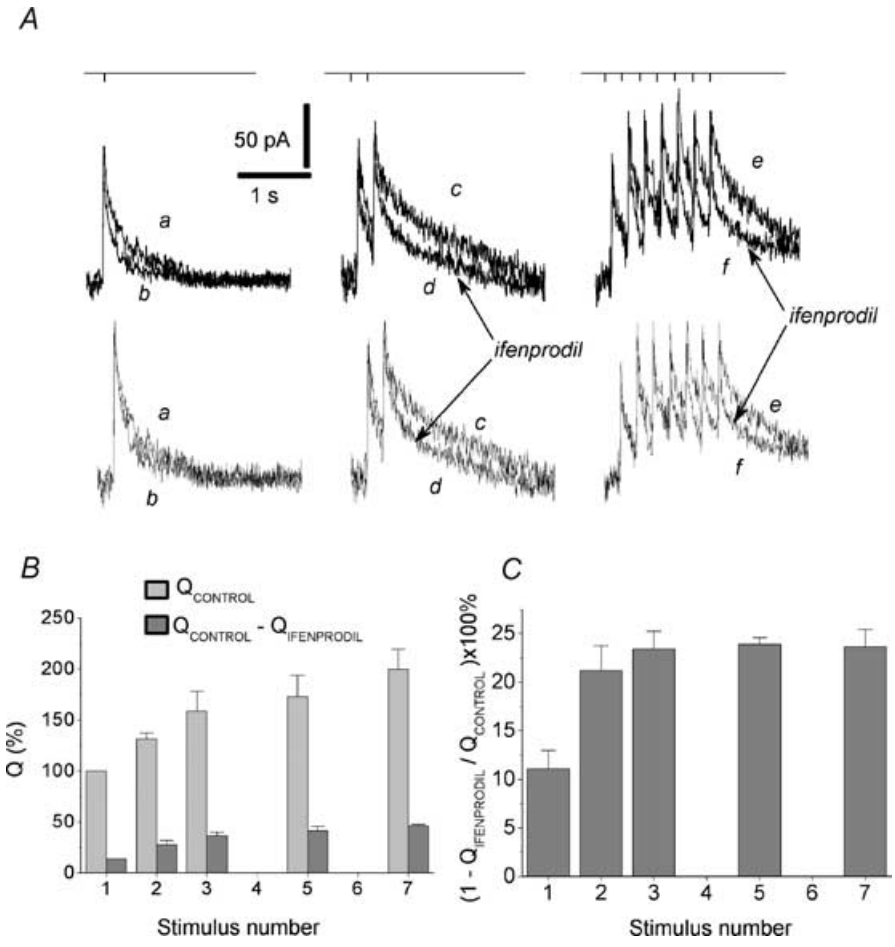

Figure 6. Increased contribution of the ifenprodil-sensitive component at theta-frequency stimulation *A*, the slow-down of $EPSC_{NMDA}$ on a spike-to-spike basis. Upper traces: $EPSC_{NMDA}$ evoked by a single pulse (traces *a* and *b*), 2 pulses (traces *c* and *d*) and 7 pulses (traces *e* and *f*); 5 Hz stimulation recorded in control solution (traces *a, c* and *e*) and in the presence of ifenprodil (traces *b, d* and *f*). Holding voltage +50 mV. Lower traces: corresponding traces normalized and superimposed. *B*, the charge transferred by the control $EPSC_{NMDA}$ and the ifenprodil-sensitive component $EPSC_{NMDA}$ ($Q_{Control} - Q_{Ifenprodil}$) evoked by a progressively increasing number of pulses (from 1 to 7) in the train (5 Hz). The control *Q* value for the $EPSC^{single}_{NMDA}$ was taken as 100%. *C*, contribution of the ifenprodil-sensitive component to the $EPSC_{NMDA}$ evoked by progressively increasing the number of pulses (from 1 to 7) in a 5 Hz train (calculated as $1 - \frac{Q_{Ifenprodil}}{Q_{Control}}$).

Fig. 4*D*). This indicates the increased contribution of ifenprodil-sensitive receptors to the peak of the afterburst EPSC.

Thus, the increase in the transmitter release by a short train of 200 Hz stimulation (which imitates the natural burst pattern) results in the involvement of 'slow' NR2B and 'superslow' NR2 D extrasynaptic receptors in the $EPSC_{NMDA}$. Figure 5*A* demonstrates the increase in the contribution of NR2B-containing receptors with the number of stimuli; saturation of the effect was observed after five to seven pulses (Fig. 5*B* and *C*).

For a given number of stimuli in the train, the higher the frequency used, the greater are both the slow-down of the $EPSC_{NMDA}$ decay and the contribution of the ifenprodil-sensitive component. Short trains of 5 Hz stimulation induced much weaker, but detectable slow-down of $EPSC_{NMDA}$ decay (Fig. 6). However, in contrast to high-frequency stimulation, the major change was detectable after the second stimulus applied at a frequency of 5 Hz.

In a separate set of experiments, pharmacologically isolated NMDA receptor-mediated field EPSPs ($EPSP_{NMDA}$) were induced by short trains of 5 Hz stimulation. We have found that the contribution of the ifenprodil-sensitive component increases with stimulus number in the train (Fig. 7). The extent of inhibition of EPSP produced by ifenprodil for the first stimulus was $52 \pm 9\%$ as compared to $71 \pm 10\%$ for the seveth stimulus ($n = 4$, $P < 0.05$). Ifenprodil only slightly altered $t_{1/2}$ of $EPSC_{NMDA}^{single}$ ($102 \pm 13\%$ of control), while $t_{1/2}$ of $EPSC_{NMDA}^{train}$ was decreased to $75 \pm 14\%$ of control values ($n = 4$; $P < 0.04$).

For hippocampus and cortex, high-frequency bursts are believed to be associated with information processing and memory consolidation. Imitation of these natural stimulus patterns is known to result in robust long-term potentiation (LTP; Dobrunz & Stevens, 1999). Some data indicate that the LTP phenomenon is accompanied by presynaptic changes, which include an increase in release probability and in the number of effective release sites (Malinow & Tsien, 1990; Bolshakov & Siegelbaum, 1995; Sokolov *et al.* 2002), but for comparison see Nicoll & Malenka (1995) and Diamond *et al.* (1998). We produced LTP in the CA1 hippocampal region by using a high-frequency stimulation (HFS) protocol (6 trains of 7 pulses each, 200 Hz). Mean post-tetanic changes comprised $210 \pm 42\%$ ($P < 0.01$, $n = 4$) for the amplitudes of field potential (data not shown) and $161 \pm 21\%$ ($P < 0.02$, $n = 5$) for the amplitude of $EPSC_{NMDA}^{single}$ (Fig. 8*A* and *D*). In this set of experiments, $EPSC_{NMDA}$ were measured in the presence of NBQX, while field potential recordings were conducted without NBQX. Pharmacologically isolated NMDA receptor-mediated synaptic responses demonstrate robust LTP (Bashir *et al.* 1991; Asztely *et al.* 1992). When measured after HFS, $EPSC_{NMDA}$ induced by a 5 Hz train displayed significant long-term slow-down of the decay, while the kinetics of the $EPSC_{NMDA}^{single}$ were only slightly altered or remained unchanged (Fig. 8*A*). The effect persisted at least for 1.5 h. In the control experiments (without HFS) no changes of the $EPSC_{NMDA}^{train}$ were observed for at least 90 min (Fig. 8*B*). Correspondingly, 60 min after HFS the relation between normalized charge transfer for the $EPSC_{NMDA}^{train}$ and $EPSC_{NMDA}^{single}$ comprised $136 \pm 13\%$ of the control values ($P < 0.07$, $n = 5$, Fig. 8*C*). The ratio of $t_{1/2}$ of $EPSC_{NMDA}^{train}$ and $t_{1/2}$ of $EPSC_{NMDA}^{single}$ was $154 \pm 25\%$ ($P < 0.05$, $n = 5$).

Discussion

We have found that pharmacological agents that preferentially inhibit slowly deactivating NMDA receptor subtypes speed up the kinetics of ultraslow afterburst EPSCs, while *D*-CPP, which is most effective against more rapid NR2A/B subunits, makes the afterburst EPSC kinetics substantially slower. In all of these cases, the kinetics of $EPSC_{NMDA}$ elicited by a single pulse remained unaffected. Among other consequences, these data indicate that the slow-down of the afterburst EPSC is not connected to the increase in the current amplitude and consequent voltage clamp and filtration problems; while the afterburst $EPSC_{NMDA}$ amplitude was inhibited in all cases, the direction of the kinetics changes depended on the pharmacological profile of the drug applied. This

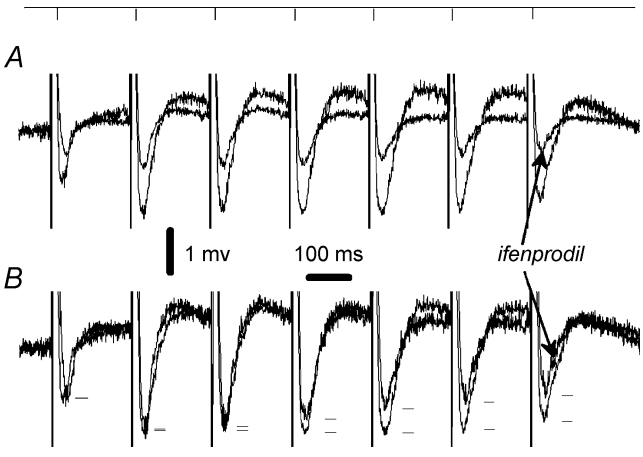

Figure 7. Pharmacologically isolated field $EPSP_{NMDA}$ measured during the course of 5 Hz stimulation

A, the traces of the $EPSP_{NMDA}$ induced by a train 7 pulses long (5 Hz) in control conditions and in the presence of 50 μM ifenprodil (superimposed). *B*, corresponding traces were normalized. The peak values of individual EPSPs are marked with dashes to demonstrate a gradual pulse-to-pulse increase in the contribution of ifenprodil-sensitive component of the signal.

observation seems to be especially important because our data indicate that the use of slowly dissociating NMDA receptor blockers for evaluating the fidelity of the voltage clamp in the *in situ* pyramidal neurones is limited by their NMDA receptor subtype specificity.

According to a recently suggested interpretation, hippocampal ultraslow EPSCs reflect spatial/temporal limitations of uptake mechanisms in conditions of synchronized neuronal activity (Arnth-Jensen *et al.* 2002). Cooperativity of densely packed CA3/CA1 synapses has been suggested as the primary consequence of these uptake limitations. Our data do not exclude a role of synaptic cross-talk in the spillover phenomenology but indicate that a substantial role in shaping the ultraslow afterburst $EPSC_{NMDA}$ belongs to the pharmacologically distinct slowly deactivating NMDA receptor subunits. Evidently, some of them become recruited very rapidly after the massive synchronized release of Glu; the contribution of the ifenprodil-sensitive component is already increased at the peak of afterburst EPSC (Fig. 4).

The following question arises: does the train stimulation activate a pool of extrasynaptic receptors or lead to the recruitment of synaptic receptors with different properties? Experiments with low-affinity competitive NMDA receptor antagonist D-aminoadipic acid (D-AA), whose efficacy depends on the concentration of glutamate (Clements *et al.* 1992) , allow distinguishing receptors activated within active synapses from those activated by spillover (Diamond, 1999) . It has been found that while leaving the kinetics of $EPSC_{NMDA}^{single}$ practically unaltered, D-AA markedly reduces the late component of $EPSC_{NMDA}^{train}$ (Grebenyuk *et al.* 2004). The present data demonstrate that the same component is inhibited by ifenprodil and PPDA.

Although numerous studies suggest synaptic localization for NMDA receptors, they are definitely also present at extrasynaptic sites (Rosenmund *et al.* 1995; Rao & Craig, 1997; Clark *et al.* 1997; Rao *et al.* 1998). Importantly, ifenprodil blocks the EPSC less effectively than the whole-cell current, which includes both synaptic and extrasynaptic receptors (Tovar & Westbrook, 1999).

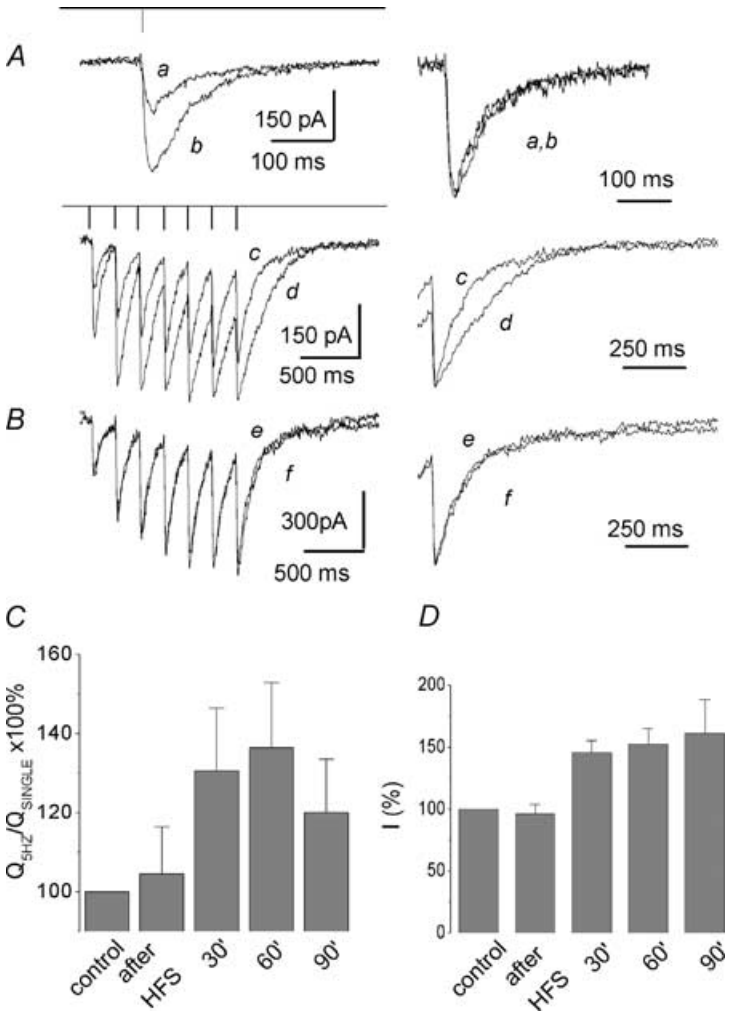

Figure 8. Long-term enhancement of the delayed component of the afterburst $EPSC_{NMDA}$ after HFS
A, left-hand traces: $EPSC_{NMDA}$ induced by single stimuli (traces *a* and *b*) and by a 5 Hz train 7 pulses long (traces *c* and *d*) before (traces *a* and *c*) and 60 min after HFS (traces *b* and *d*). HFS stimulation protocol was as follows: train 7 pulses long (200 Hz) was applied 6 times with 20 s intervals. Holding voltage was −45 mV. Right-hand traces: corresponding $EPSC_{NMDA}$ scaled to the same amplitude and superimposed as indicated. *B*, control experiment demonstrating the lack of slow-down of the $EPSC_{NMDA}^{train}$ in the course of long-term measurements (90 min) in the absence of HFS. The $EPSC_{NMDA}$ induced by a train (5 Hz) 7 pulses long before (trace *e*) and after 90 min of the whole-cell recording (trace *f*). Both traces exactly coincide, as seen in the normalized superposition at a higher sweep speed (right-hand traces). *C*, train-to-single ratio of the normalized charge to the peak charge transfer measured in control conditions, immediately after HFS and successively at 30, 60 and 90 min after HFS (calculated as $\frac{Q_{5Hz}}{Q_{Single}}$). *D*, averaged amplitude of the $EPSC_{NMDA}$ induced by single stimulus measured in control conditions, immediately after, and at 30, 60 and 90 min after HFS.

Non-synaptic NMDA receptor clusters have been reported to be prominent in developing cortical tissue, some of them remaining intracellular and some being associated with the plasma membrane (Aoki *et al.* 1994; Johnson *et al.* 2003). NMDA receptor clusters non-colocalized with presynaptic markers were detected in numerous studies using cultured hippocampal neurones and immunocytochemical methods (Aoki *et al.* 1994; Liao *et al.* 1999; Pickard *et al.* 2000). Recent evidence suggests that NMDA receptors are highly dynamic and can move laterally between synaptic and extrasynaptic pools (Tovar & Westbrook, 2002). Distinct regulation of synaptic *versus* extrasynaptic NMDA receptors has been reported (Li *et al.* 2002); Ca^{2+} and tyrosine phosphorylation differentially regulate run-down of synaptic *versus* extrasynaptic NMDA receptor-mediated current in rat hippocampal pyramidal neurones, providing mechanisms for receptor adaptation to a variety of stimuli. Furthermore, varying cellular consequences of NMDA receptor activation ((cAMP response element binding protein) CREB function, gene regulation and neurone survival)) were specified for the synaptic *versus* extrasynaptic location of the receptors activated in cultured hippocampal neurones (Hardingham *et al.* 2002).

At present it is not known which di- and/or triheteromeric NR2D-containing NMDA receptor assemblies are expressed in hippocampus *in vivo* and how the inclusion of NR2D in such assemblies affects distinct single-channel properties. Immunohistochemical data suggest that all NR2D-containing receptors in the adult midbrain may be triheteromeric (Dunah *et al.* 1998). The expression of NR1/NR2D and NR1/NR2B/NR2D assemblies has been demonstrated recently in cerebellar Golgi cells (Brickley *et al.* 2003). The triheteromeric NR1/NR2B/NR2D assembly generates channels with properties distinct from NR2B and NR2D, in particular, with intermediate sensitivity to ifenprodil. Therefore, at present it is difficult to specify whether the ifenprodil-sensitive component of $EPSC_{NMDA}$ recorded in our experiments corresponds to pure NR2B or NR2B-containing receptor assemblies.

We demonstrate here that robust LTP, produced by repetitive high-frequency stimulation, is accompanied by a long-term increase in the contribution of extrasynaptic NMDA receptors to the aftertrain EPSC. The increased contribution of extrasynaptic receptors after HFS could be a result of the long-term increase in glutamate release that has been shown to occur in CA3/CA1 synapses after induction of LTP (Malinow & Tsien, 1990; Bolshakov & Siegelbaum, 1995; Sokolov *et al.* 2002), though modification in glutamate uptake machinery cannot be excluded. Plasticity involving extrasynaptic NMDA receptors could be important for memory consolidation processes, that, according to the 'synaptic re-entry reinforcement hypothesis', require multiple rounds of NMDA receptor-dependent modification to reinforce the synaptic changes initiated during memory acquisition (Shimizu *et al.* 2000; Wittenberg & Tsien, 2002). Experiments with Ca^{2+} imaging reveal that NMDA receptors play a leading role in creating the postsynaptic Ca^{2+} signal (Kovalchuk *et al.* 2000). NR2B receptors have a higher Ca^{2+} permeability than NR2A (Dingledine *et al.* 1999). The enhancement of their activity on a spike-to-spike basis may well account for the ability of bursts to make synaptic transmission reliable and to cause plasticity (Lisman, 1997). In particular, the NR2B subunit has been suggested to have a critical role in spatial learning and LTP, as evidenced by NR2B knockout and overexpressing mice (Sprengel *et al.* 1998; Tang *et al.* 1999; Tovar *et al.* 2000). Tang *et al.* (1999) showed that mice in which the NR2B subunit of the NMDA receptor is overexpressed display a striking increase in synaptic plasticity and learning ability. A role for NR2D in hippocampal long-term depression (LTD) has been recently proposed (Hrabetova *et al.* 2000).

In summary, our data indicate that the phenomenon of 'ultraslow' $EPSC_{NMDA}$ comprises the recruitment of ultraslow NMDA receptor subtypes. Their extrasynaptic location indicates that spillover results in the activation of non-synaptic routes of calcium entry into the dendrite. Correspondingly, the stimulus dependence of the $EPSC_{NMDA}$ kinetics can reflect a confluence of transmitter over extrasynaptic spaces. Taking into account independent compartmentalization of spines and extrasynaptic intracellular calcium pools (Yuste & Tank, 1996; Sabatini *et al.* 2001), the kill as large as the loss of synaptic specificity may become unnecessary . To answer the question of how much genuine intersynaptic cross-talk is involved, one needs more specific pharmacological tools and/or other approaches. Evidently, as for the consequences of spillover for synaptic plasticity, a more 'complicated scenario' (Diamond, 2002) is needed for their interpretation; the role(s) of intradendritic calcium should be considered.

References

Aoki C, Venkatesan C, Go CG, Mong JA & Dawson TM (1994). Cellular and subcellular localization of NMDA-R1 subunit immunoreactivity in the visual cortex of adult and neonatal rats. *J Neurosci* **14**, 5202–5222.

Arnth-Jensen N, Jabaudon D & Scanziani M (2002). Cooperation between independent hippocampal synapses is controlled by glutamate uptake. *Nat Neurosci* **5**, 325–331.

Asztely F, Erdemli G & Kullmann DM (1997). Extrasynaptic glutamate spillover in the hippocampus: dependence on temperature and the role of active glutamate uptake. *Neuron* **18**, 281–293.

Asztely F, Wigstrom H & Gustafsson B (1992). The relative contribution of NMDA receptor channels in the expression of long-term potentiation in the hippocampal CA1 region. *Eur J Neurosci* **4**, 681–690.

Bashir ZI, Alford S, Davies SN, Randall AD & Collingridge GL (1991). Long-term potentiation of NMDA receptor-mediated synaptic transmission in the hippocampus. *Nature* **349**, 156–158.

Beaton JA, Stemsrud K & Monaghan DT (1992). Identification of a novel *N*-methyl-D-aspartate receptor population in the rat medial thalamus. *J Neurochem* **59**, 754–757.

Bolshakov VY & Siegelbaum SA (1995). Regulation of hippocampal transmitter release during development and long-term potentiation. *Science* **269**, 1730–1734.

Brickley SG, Misra C, Mok MH, Mishina M & Cull-Candy SG (2003). NR2B and NR2D subunits coassemble in cerebellar Golgi cells to form a distinct NMDA receptor subtype restricted to extrasynaptic sites. *J Neurosci* **23**, 4958–4966.

Buller AL, Larson HC, Schneider BE, Beaton JA, Morrisett RA & Monaghan DT (1994). The molecular basis of NMDA receptor subtypes: native receptor diversity is predicted by subunit composition. *J Neurosci* **14**, 5471–5484.

Buller AL & Monaghan DT (1997). Pharmacological heterogeneity of NMDA receptors: characterization of NR1a/NR2D heteromers expressed in *Xenopus* oocytes. *Eur J Pharmacol* **320**, 87–94.

Clark BA, Farrant M & Cull-Candy SG (1997). A direct comparison of the single-channel properties of synaptic and extrasynaptic NMDA receptors. *J Neurosci* **17**, 107–116.

Clements JD, Lester RA, Tong G, Jahr CE, Westbrook GL (1992). The time course of glutamate in the synaptic cleft. *Science* **258**, 1498–1501.

Cull-Candy S, Brickley S & Farrant M (2001). NMDA receptor subunits: diversity, development and disease. *Curr Opin Neurobiol* **11**, 327–335.

Cull-Candy SG, Brickley SG, Misra C, Feldmeyer D, Momiyama A & Farrant M (1998). NMDA receptor diversity in the cerebellum: identification of subunits contributing to functional receptors. *Neuropharmacology* **37**, 1369–1380.

Diamond JS (2001). Neuronal glutamate transporters limit activation of NMDA receptors by neurotransmitter spillover on CA1 pyramidal cells. *J Neurosci* **21**, 8328–8338.

Diamond JS (2001). Neuronal glutamate transporters limit activation of NMDA receptors by neurotransmitter spillover on CA1 pyramidal cells. *J Neurosci* **21**, 8328–8338.

Diamond JS (2002). A broad view of glutamate spillover. *Nat Neurosci* **5**, 291–292.

Diamond JS, Bergles DE & Jahr CE (1998). Glutamate release monitored with astrocyte transporter currents during LTP. *Neuron* **21**, 425–433.

Dingledine R, Borges K, Bowie D & Traynelis SF (1999). The glutamate receptor ion channels. *Pharmacol Rev* **51**, 7–61.

Dobrunz LE & Stevens CF (1999). Response of hippocampal synapses to natural stimulation patterns. *Neuron* **22**, 157–166.

Dunah AW, Luo J, Wang YH, Yasuda RP & Wolfe BB (1998). Subunit composition of *N*-methyl-D-aspartate receptors in the central nervous system that contain the NR2D subunit. *Mol Pharmacol* **53**, 429–437.

Durand GM, Gregor P, Zheng X, Bennett MV, Uhl GR & Zukin RS (1992). Cloning of an apparent splice variant of the rat *N*-methyl-D-aspartate receptor NMDAR1 with altered sensitivity to polyamines and activators of protein kinase C. *Proc Natl Acad Sci U S A* **89**, 9359–9363.

Grebenyuk S, Lozovaya N, Tsintsadze T & Krishtal O (2004). Post-synaptic NMDA signalling in hippocampal neurons of rat: spillover increases the impact of each spike in a short burst discharge. *Neuroscience Letters*. **367**, 60–66.

Hardingham GE, Fukunaga Y & Bading H (2002). Extrasynaptic NMDARs oppose synaptic NMDARs by triggering CREB shut-off and cell death pathways. *Nat Neurosci* **5**, 405–414.

Hrabetova S, Serrano P, Blace N, Tse HW, Skifter DA, Jane DE *et al.* (2000). Distinct NMDA receptor subpopulations contribute to long-term potentiation and long-term depression induction. *J Neurosci* **20**, RC81:1–6.

Ikeda K, Nagasawa M, Mori H, Araki K, Sakimura K, Watanabe M *et al.* (1992). Cloning and expression of the epsilon 4 subunit of the NMDA receptor channel. *FEBS Lett* **313**, 34–38.

Johnson RR, Jiang X & Burkhalter A (2003). Regional and laminar differences in synaptic localization of NMDA receptor subunit NR1 splice variants in rat visual cortex and hippocampus. *J Comp Neurol* **368**, 335–355.

Kandel ER & Spencer WA (1961). Electrophysiology of hippocampal neurons. II. After-potentials and repetitive firing. *J Neurophysiol* **24**, 243–259.

Kew JN, Richards JG, Mutel V & Kemp JA (1998). Developmental changes in NMDA receptor glycine affinity and ifenprodil sensitivity reveal three distinct populations of NMDA receptors in individual rat cortical neurons. *J Neurosci* **18**, 1935–1943.

Kirson ED, Schirra C, Konnerth A & Yaari Y (1999). Early postnatal switch in magnesium sensitivity of NMDA receptors in rat CA1 pyramidal cells. *J Physiol* **521**, 99–111.

Kirson ED & Yaari Y (1996). Synaptic NMDA receptors in developing mouse hippocampal neurones: functional properties and sensitivity to ifenprodil. *J Physiol* **497**, 437–455.

Kovalchuk Y, Eilers J, Lisman J & Konnerth A (2000). NMDA receptor-mediated subthreshold Ca^{2+} signals in spines of hippocampal neurons. *J Neurosci* **20**, 1791–1799.

Kutsuwada T, Kashiwabuchi N, Mori H, Sakimura K, Kushiya E, Araki K *et al.* (1992). Molecular diversity of the NMDA receptor channel. *Nature* **358**, 36–41.

Li B, Chen N, Luo T, Otsu Y, Murphy TH & Raymond LA (2002). Differential regulation of synaptic and extra-synaptic NMDA receptors. *Nat Neurosci* **5**, 833–834.

Liao D, Zhang X, O'Brien R, Ehlers MD & Huganir RL (1999). Regulation of morphological postsynaptic silent synapses in developing hippocampal neurons. *Nat Neurosci* **2**, 37–43.

Lisman JE (1997). Bursts as a unit of neural information: making unreliable synapses reliable. *Trends Neurosci* **20**, 38–43.

Lozovaya NA, Kopanitsa MV, Boychuk YA & Krishtal OA (1999). Enhancement of glutamate release uncovers spillover-mediated transmission by *N*-methyl-D-aspartate receptors in the rat hippocampus. *Neuroscience* **91**, 1321–1330.

Malinow R & Tsien RW (1990). Presynaptic enhancement shown by whole-cell recordings of long-term potentiation in hippocampal slices. *Nature* **346**, 177–180.

Momiyama A, Feldmeyer D & Cull-Candy SG (1996). Identification of a native low-conductance NMDA channel with reduced sensitivity to Mg^{2+} in rat central neurones. *J Physiol* **494**, 479–492.

Monyer H, Burnashev N, Laurie DJ, Sakmann B & Seeburg PH (1994). Developmental and regional expression in the rat brain and functional properties of four NMDA receptors. *Neuron* **12**, 529–540.

Nicoll RA & Malenka RC (1995). Contrasting properties of two forms of long-term potentiation in the hippocampus. *Nature* **377**, 115–118.

Pickard L, Noel J, Henley JM, Collingridge GL & Molnar E (2000). Developmental changes in synaptic AMPA and NMDA receptor distribution and AMPA receptor subunit composition in living hippocampal neurons. *J Neurosci* **20**, 7922–7931.

Rank JB (1973). Studies on single neurons in dorsal hippocampal formation and septum in unrestrained rats. 1. Behavioral correlates and firing repertoires. *Exp Neurol* **41**, 462–531.

Rao A & Craig AM (1997). Activity regulates the synaptic localization of the NMDA receptor in hippocampal neurons. *Neuron* **19**, 801–812.

Rao A, Kim E, Sheng M & Craig AM (1998). Heterogeneity in the molecular composition of excitatory postsynaptic sites during development of hippocampal neurons in culture. *J Neurosci* **18**, 1217–1229.

Rosenmund C, Feltz A & Westbrook GL (1995). Synaptic NMDA receptor channels have a low open probability. *J Neurosci* **15**, 2788–2795.

Sabatini BL, Maravall M & Svoboda K (2001). Ca^{2+} signaling in dendritic spines. *Curr Opin Neurobiol* **11**, 349–356.

Scherzer CR, Landwehrmeyer GB, Kerner JA, Counihan TJ, Kosinski CM, Standaert DG *et al.* (1998). Expression of *N*-methyl-D-aspartate receptor subunit mRNAs in the human brain: hippocampus and cortex. *J Comp Neurol* **390**, 75–90.

Shimizu E, Tang Y, Rampon I & Tsien JZ (2000). NMDA receptor-dependent synaptic reinforcement as a crucial process for memory consolidation. *Science* **290**, 1170–1174.

Sokolov MV, Rossokhin AV, Astrelin AV, Frey JU & Voronin LL (2002). Quantal analysis suggests strong involvement of presynaptic mechanisms during the initial 3 h maintenance of long-term potentiation in rat hippocampal CA1 area *in vitro*. *Brain Res* **957**, 61–75.

Sprengel R, Suchanek B, Amico C, Brusa R, Burnashev N, Rozov A *et al.* (1998). Importance of the intracellular domain of NR2 subunits for NMDA receptor function *in vivo*. *Cell* **92**, 279–289.

Suzuki SS & Smith GK (1985). Burst characteristics of hippocampal complex spike cells in the awake rat. *Exp Neurol* **89**, 90–95.

Tang YP, Shimizu E, Dube GR, Rampon C, Kerchner GA, Zhuo M *et al.* (1999). Genetic enhancement of learning and memory in mice. *Nature* **401**, 63–69.

Thompson CL, Drewery DL, Atkins HD, Stephenson FA & Chazot PL (2002). Immunohistochemical localization of *N*-methyl-D-aspartate receptor subunits in the adult murine hippocampal formation: evidence for a unique role of the NR2D subunit. *Brain Res Mol Brain Res* **102**, 55–61.

Tovar KR, Sprouffske K & Westbrook GL (2000). Fast NMDA receptor-mediated synaptic currents in neurons from mice lacking the epsilon2 (NR2B) subunit. *J Neurophysiol* **83**, 616–620.

Tovar KR & Westbrook GL (1999). The incorporation of NMDA receptors with a distinct subunit composition at nascent hippocampal synapses in vitro. *J Neurosci* **19**, 4180–4188.

Tovar KR & Westbrook GL (2002). Mobile NMDA receptors at hippocampal synapses. *Neuron* **34**, 255–264.

Vicini S, Wang JF, Li JH, Zhu WJ, Wang YH, Luo JH *et al.* (1998). Functional and pharmacological differences between recombinant *N*-methyl-D-aspartate receptors. *J Neurophysiol* **79**, 555–566.

Williams K (1993). Ifenprodil discriminates subtypes of the *N*-methyl-D-aspartate receptor: selectivity and mechanisms at recombinant heteromeric receptors. *Mol Pharmacol* **44**, 851–859.

Wittenberg GM & Tsien JZ (2002). An emerging molecular and cellular framework for memory processing by the hippocampus. *Trends Neurosci* **25**, 501–505.

Wyllie DJ, Behe P & Colquhoun D (1998). Single-channel activations and concentration jumps: comparison of recombinant NR1a/NR2A and NR1a/NR2D NMDA receptors. *J Physiol* **510**, 1–18.

Yuste R & Tank DW (1996). Dendritic integration in mammalian neurons, a century after Cajal. *Neuron* **16**, 701–716.

Acknowledgements

This work was supported by the Wellcome Trust, Howard Hughes Medical Institute and RO1 MH60252 grants.